Stark-modulation spectroscopy of the $B(1)[^3\Pi]$ state of PbO

D. Kawall,* Y. V. Gurevich, C. Cheung, S. Bickman, Y. Jiang, and D. DeMille

Department of Physics, Yale University, P.O. Box 208120, New Haven, Connecticut 06520-8120 USA

We report detailed spectroscopic measurements of the $X(0)[^1\Sigma^+](v=0)\rightarrow B(1)[^3\Pi](v=5)$ transition in PbO. Using a Stark-modulated laser absorption technique, we have measured the hyperfine constant of ^{207}PbO in the $B(1)$ state, as well as the $B(1)(v=5)$ rotational constant, X-B isotope shifts, etc. The hyperfine constant of the $B(1)$ state is of interest as a benchmark for calculations of PbO electronic structure related to experiments to search for the electric dipole moment of the electron.

PACS number(s): 33.15.−e, 33.20.Kf, 14.60.Cd

Spectroscopy of the PbO molecule has become of interest since it is a good candidate for use in searches for a permanent electric dipole moment (EDM) of the electron, d_e. EDMs are interesting because a nonzero value for an EDM of any fundamental particle would violate parity and time-reversal symmetries. Standard model predictions for EDMs are well below any proposed experimental sensitivities. However, most extensions of the standard model predict dramatically enhanced EDMs.

A promising approach toward improving the limits on d_e involves heavy polar diatomic molecules in a configuration with an unpaired electron spin. In such systems, the effective electric field W_d seen by the unpaired electron can be many orders of magnitude larger than external fields attainable in the laboratory [1,2]. An electron EDM can be detected by spin polarizing an electron along this internal field and searching for the characteristic linear Stark shift $\Delta E = -d_e W_d$. Interpreting experimental limits on ΔE measured in a molecule in terms of d_e requires a value for W_d. This can be obtained using semiempirical wave functions for the state of interest [1] or from *ab initio* calculations [2]. Spectroscopic properties sensitive to the electron spin density at the nucleus such as hyperfine structure (hfs) can constrain the parameters in semiempirical evaluations of W_d or test the predictions of *ab initio* calculations.

An experiment is underway in our laboratory using the $a(1)[^3\Sigma^+]$ state of PbO that may improve the current limit $|d_e| < 1.6 \times 10^{-27} e$ cm [3] by several orders of magnitude [4]. Such an improvement would probe large regions of the parameter space of many standard model extensions. Stimulated by this work, a measurement of the hyperfine constant of the $a(1)$ state was recently reported [5]. The hfs of the $B(1)[^3\Pi]$ state of ^{207}PbO is also of interest, since it can be used to further check and/or refine the electronic structure calculations used to calculate the value of W_d in the $a(1)$ state. In addition, knowledge of the $B(1)$ hfs can be used for estimating W_d for the $B(1)$ state, which also may be a viable candidate for an EDM search [6]. This motivates this effort to determine the hfs of the $B(1)$ state of PbO.

The measurements were made by observing the absorption of laser light by PbO vapor in a cell as the laser wavelength was tuned. The cell contains a PbO of natural isotopic abundance; it is constructed from a 5.7 cm cube of alumina, with a 5.1 cm diameter through holes bored perpendicular to, and centered on, each face. The top and bottom holes of the resulting cubical frame structure are capped with alumina plates. Thin yttrium aluminum garnet (YAG) windows are bonded on the remaining four holes using gold foil as an intermediate layer. The cell is heated to 700 °C by the radiation from resistively heated thin foils of tantalum supported on a quartz framework surrounding the cell. This results in a PbO number density $n \approx 4 \times 10^{13}$ cm^{-3} in the cell. The laser used in the measurements was an external cavity diode system based on a standard design [7]. Our system used a Nichia NLHV500C violet diode laser and 3600 grooves/mm diffraction grating in a Littrow configuration. The laser provided $\lesssim 1$ mW of power around 406.5 nm which passed through the YAG windows into the cell.

To enable sensitive lock-in detection of the absorption, we employed a Stark modulation technique [8]. As explained below, this method enhances signals from low J levels where the hfs is largest, which are otherwise difficult to isolate within the spectrally congested region near the bandhead. Here we briefly discuss the basic features of the Stark-modulated signals, as relevant to our experiment.

The Stark effect in the $X(0) \rightarrow B(1)$ transition is dominated by shifts due to mixing between the closely spaced Ω-doublet levels in the $B(1)$ state. The doublet members, e and f, share a common value of total (electronic +rotational) angular momentum **J** but are of opposite parity. The spacing between the doublet levels is given by $\Delta_\Omega(J) = qJ(J+1)$, where $q \ll B_{v=5}$, and $B_{v=5}$ is the rotational constant of the $B(1)(v=5)$ state. [By convention, q is positive if the e level, with parity $P=(-1)^J$, is at a higher energy.] In the absence of an electric field **E**, selection rules for the electric-dipole $X \rightarrow B$ transition ensure that the laser light is absorbed only in the transition to one of the doublet levels. In the presence of **E**, the e and f levels mix and are shifted by an amount $\Delta \nu$ given by

$$\Delta \nu = \pm \left[\sqrt{[\Delta_\Omega(J)/2]^2 + (\alpha E)^2} - \Delta_\Omega(J)/2 \right]. \quad (1)$$

Here the upper (lower) sign corresponds to the upper (lower) level in the limit $E \rightarrow 0$, and

*Present addresses: Department of Physics, University of Massachusetts, Amherst, MA 01003 and RIKEN-BNL Research Center, Upton, NY 11973.
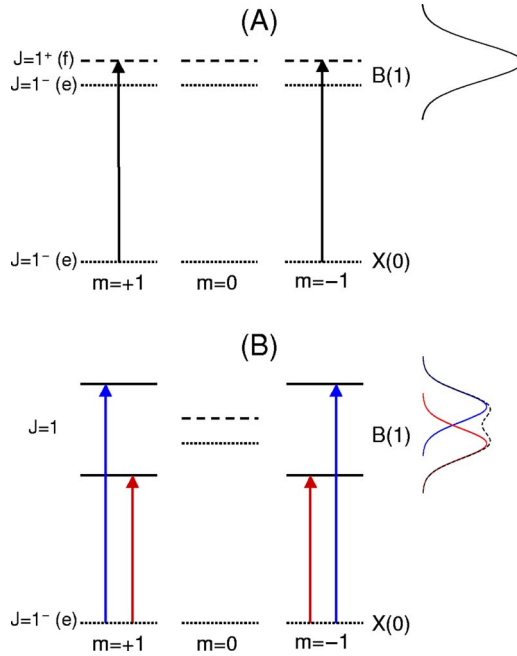
FIG. 1. (Color online) Stark modulation of the excited state energy levels, leading to a modulation of the transmitted light intensity. Plot (A) shows the $Q1$ transition and the absorption expected at $E=0$. In (B), with E large, the Stark effect mixes and shifts the doublet levels. The difference in absorption is recorded in the scans.

$$\alpha = \mu_{B(1)} M_F \frac{F(F+1) + J(J+1) - I(I+1)}{2F(F+1)J(J+1)}, \qquad (2)$$

where $\mu_{B(1)}$ is the dipole moment of the B state, and $F=J+I$ is the total angular momentum. In the limit of large E and small J, $\Delta\nu \propto E$ and the doublet levels are completely mixed. In this limit, the laser is absorbed with equal strength by both eigenstates of the mixed doublet, and the repulsion of the doublet levels results in a characteristic broadening of the absorption spectral line (see Fig. 1). For a laser tuned to one of the unperturbed doublet levels, by modulating $\mathbf{E}$, maxima in absorption will occur twice per period at the minima of E. The Ω-doublet mixing leads to small shifts in the line centers, as does the slight residual Stark mixing with nearby rotational levels of opposite parity. Both of these small shifts ($\lesssim 50$ MHz) are accounted for in the analysis.

In our measurements, an electric field $\mathbf{E}$ was produced using two parallel 3.8 cm diameter gold foil electrodes spaced 0.6 cm apart in the cell. The laser light was linearly

polarized parallel to $\mathbf{E}$ and traversed the vapor cell between the electrodes. A reference signal at $\omega = 2\pi \times 99$ kHz was amplified to produce a voltage $V = V_0 \cos(\omega t)$, where $V_0 \approx 800$ V, across the electrodes. The transmitted light was detected with a photodiode and amplified. Part of the laser beam was diverted for a wavelength measurement (using a Burleigh WA-1500 Wavemeter), and the laser power reflected from the cell was monitored with a second "reference" photodiode.

The transmitted signals were sampled at 1 MHz with a 12 bit analog-to-digital converter and recorded for 4 s. The amplitude of the signal at the second harmonic of the reference was extracted from the digitized data. Then the laser frequency was advanced roughly 150 MHz by simultaneous adjustment of the grating angle and diode current, and an absorption measurement was taken. This cycle was repeated until a mode hop occurred yielding scans covering 15–30 GHz.

The scans showed absorption features corresponding to ^{208}PbO, ^{207}PbO, and ^{206}PbO molecules making P-, Q-, and R-branch transitions from the electronic ground state $X(0)$ $\times [^1\Sigma^+](v''=0, J'')$ to the excited state $B(1)[^3\Pi](v'=5, J')$, with $S/N \gtrsim 1$ for $J''=0-6$. An example is shown in Fig. 2. Before analyzing the data, the absorption amplitudes were corrected for the variation in laser power with frequency during a scan. We expect residual variations in amplitude over the scan of $\sim 5\%$, based on observed fluctuations in the ratio between transmitted and reflected power (presumably due to interference effects in the cell windows). The statistical uncertainty in each measurement was estimated from the fluctuations of the second harmonic out of phase with the signal, and was typically a few times greater than the shot noise in the photodiode signal. The largest signal was observed from the $Q1$ ^{208}PbO line, with a peak $S/N \gtrsim 75$, corresponding to ≈ 4 ppm absorption. These scans were fit to extract the hfs constant and coefficients in the Dunham expansion as described below.

Hyperfine structure in the $B(1)$ state of ^{207}PbO arises from the interaction $H_{\text{hfs}} = \mathbf{J}_e \cdot \mathbf{A} \cdot \mathbf{I} = A_\parallel J_{eZ} I_Z + A_\perp (J_{eX} I_X + J_{eY} I_Y)$, where $\mathbf{A}$ is the hyperfine tensor, $I=1/2$ is the nuclear spin of ^{207}Pb, $\mathbf{J}_e$ is the electronic angular momentum, and the coordinate axes are defined in the body-fixed frame, with $\hat{Z}$ along the internuclear axis $\hat{n}$. For levels with low J values in an $\Omega = 1$ electronic state, the hfs is dominated by the term in H_{hfs} proportional to $A_\parallel$. The terms containing $J_{X,Y}$ induce off-diagonal mixing with states with $\Omega \neq 1$, which are far in energy for this Hund's case (c) molecular state. We can thus write the energy shift due to hfs, correct to second order in $H_{\text{hfs}} \approx A_\parallel J_{eZ} I_Z$, as
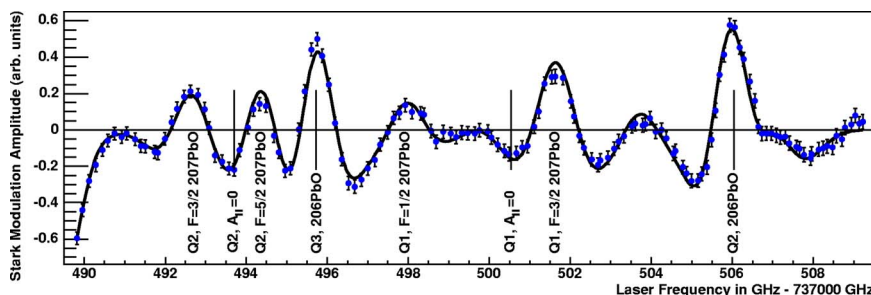

FIG. 2. (Color online) Segment of a typical Stark modulation scan. The points are data and the line is a fit. The vertical bars mark the line centers in the absence of hfs; the hyperfine splitting of the ^{207}PbO lines is clearly visible.

$$\Delta E_{\rm hfs} \approx \langle FIJM_F\Omega|A_\|J_{eZ}I_Z|FIJM_F\Omega\rangle$$
$$+ \sum_{J'=J\pm1} \frac{|\langle FIJ'M_F\Omega|A_\|J_{eZ}I_Z|FIJM_F\Omega\rangle|^2}{E_{FIJ} - E_{FIJ'}}. \quad (3)$$

The matrix elements are determined from

$$\langle FIJ'M_F\Omega|J_{eZ}I_Z|FIJM_F\Omega\rangle$$
$$= (-1)^{F+I+J}\begin{Bmatrix} F & I & J' \\ 1 & J & I \end{Bmatrix}\sqrt{I(I+1)(2I+1)}$$
$$\times(-1)^{J'-\Omega}\sqrt{(2J'+1)(2J+1)}\begin{pmatrix} J' & 1 & J \\ -\Omega & 0 & \Omega \end{pmatrix}\Omega. \quad (4)$$

Equation (3) then simplifies to

$$\Delta E_{\rm hfs}^{F=J\pm1/2} = \pm\frac{A_\|}{2(F+1/2)} \mp \frac{A_\|^2}{8B_{v=5}}\frac{(F-1/2)(F+3/2)}{(F+1/2)^3}. \quad (5)$$

Initial assignments of each line were possible using estimates of the $B(1)$ state energies by extrapolation from the data of Ref. [9], and taking into account the known natural abundances of each Pb isotope. The line splitting due to hfs in ^{207}PbO is clearly visible in two transitions, corresponding to the $Q1$ and $Q2$ lines, in Fig. 2. The unperturbed line positions of these hfs-split lines could be located initially by extrapolating from ^{207}PbO lines with higher values of J, which exhibit much smaller hfs splitting. The sign of $A_\|$ is found to be positive by visual inspection of Fig. 2, using the following observations: the largest peak, which is closest to the unperturbed line center, must arise from the $F=J+1/2$ state [see Eq. (5)]; and in addition, if $A_\|>0$ (<0), then this line should lie higher (lower) in energy than the unperturbed line center.

Once the lines were assigned, each scan was analyzed with a multiparameter fit in which the modulated absorption lines were approximated as a sum over second derivatives of a Gaussian, with a separate Gaussian for each value of m_J in the excited state. With the isotopic abundances fixed, several fit parameters were used to characterize the height and the width of the various transitions; these included the ratio of $P:Q$ and $R:Q$ transition strengths, the value of $\mu_{B(1)}$, the Doppler width, and a measure of the electric field inhomogeneity. To extract line positions, the energy $E^{Z,A}(v,J)$ of electronic state Z ($Z=X,B$) with vibrational and rotational quantum numbers v and J, respectively, for the ^{A}PbO isotopic species was written as

$$E^{Z,A}(v,J) = G_v^{Z,A} + B_v^{Z,A}J(J+1) - D_v^{Z,A}J^2(J+1)^2$$
$$+ E^{X,A}(v=0,J=0). \quad (6)$$

The energies of the X state sublevels were taken from the precise data of Refs. [9–12]. The B state values were determined by fitting with separate values of the rotational constants used for the Ω-doublet levels with e and f character. For ^{207}PbO, the hfs constant $A_\|$ was included as an additional fit parameter.

TABLE I. Dunham coefficients $Y_{ij}^{B,208}$, in cm^{-1}. The value given in the place for Y_{00} is actually T_e+Y_{00}.

$i\backslash j$	0	1
0	22282.4297(60)	0.26465(1)
1	498.497(13)	−0.002561(12)
2	−2.331(63)	−3.4(4)×10^{-5}
3	0.03638(80)	

As described above, determination of $A_\|$ was the primary goal of our work. Fitting the data set yielded $A_\|=5.01(7)$ GHz, where the dominant uncertainty is from the spread in the fit results from different scans, with smaller contributions from variations in the fit results from changes in the laser power correction and other input parameters. This value is in good agreement with the *ab initio* prediction in [2]. We also find $G_{v=5}^{B,208}=24\,600.085(8)$ cm^{-1}, (where the uncertainty is from the wavemeter absolute calibration specification, which we did not verify independently, and from the extraction of the line centers), $B_{v=5}^{B,208}=0.249\,39(20)$ cm^{-1}, and $\mu_{B(1)}=4(1)$ D. Our data is insensitive to the small parameters $D_{v=5}^{B,208}$ and q.

The shifts between the values of $G_{v=5}^{B,A}$ for the different isotopes arise from changes in both the rovibrational and electronic energies. In order to separate these effects, it is necessary to evaluate the absolute rovibrational energies of the $B(1)(v=5)$ and the $X(0)(v=0)$ states. We accomplish this using a Dunham expansion

$$E^{Z,A}(v,J) = T_e^{Z,A} + \sum_{j,k} Y_{jk}^{Z,A}(v+1/2)^j[J(J+1)]^k. \quad (7)$$

Here the isotopic changes in rovibrational energy are taken into account by writing $Y_{jk}^{Z,A}=Y_{jk}^{Z,208}\rho_A^{-(j/2+k)}$, where $\rho_A\equiv\mu(A)/\mu(208)$ and $\mu(A)$ is the molecular reduced mass of ^{A}PbO. The coefficients in the Dunham expansion are simply related to the previously described parameters. For example, $G_{v=5}^{B,A}=T_e^{B,A}+\Sigma_j Y_{j0}^{B,A}(5+1/2)^j-\Sigma_j Y_{j0}^{X,A}(0+1/2)^j$.

To evaluate the rovibronic part of the isotopic shifts, we take the values of $Y_{jk}^{X,208}$ from Ref. [9]. The Dunham coefficients $Y_{jk}^{B,208}$ given in Table I were evaluated using the data of Ref. [9] on the three lowest vibrational levels ($v=0,1,2$) of the $B(1)$ state, in combination with our determination of $G_{v=5}^{B,208}$ and $B_{v=5}^{B,208}$. Although inclusion of our data shifts the values of individual Dunham coefficients noticeably (as compared to their values using only the data from Ref. [9]), the resulting change in the rovibronic part of the isotope shifts is small, $\lesssim100$ MHz, comparable to the uncertainty in our determination of individual line positions. Due to our limited range in J, we have negligible sensitivity to isotopic differences in the rotational constants.

With this determination of the rovibronic part of the isotope shift it is possible to extract the isotopic shifts in the electronic energies. Defining $\Delta\nu(A-A')\equiv(T_e^{B,A}-T_e^{X,A})-(T_e^{B,A'}-T_e^{X,A'})$, we find $\Delta\nu(208-207)=-270(50)$ MHz and $\Delta\nu(208-206)=-720(60)$ MHz. In a second approach, line centers from two different isotopes were extracted with no

constraints on their relative positions or amplitudes. Subtracting off the rovibronic part of the separation expected between the lines from Eq. (7) gave consistent results for the electronic part of the isotope shifts. To account for these electronic shifts, we write

$$T_e^{Z,A} = T_e^{Z,P}\left(1 + V^Z\langle r_A^2\rangle + \Delta^Z\frac{m_e}{M_A}\right). \qquad (8)$$

In this expression, $T_e^{Z,P}$ is the electronic energy of state Z for a hypothetical pointlike nucleus of infinite mass, and the parameters V^Z and Δ^Z characterize the field shift and mass shift parts, respectively, of the electronic isotope shift [13,14]; here $\langle r_A^2\rangle$ and M_A are the mean-square charge radius and the mass, respectively, of the ^{A}Pb nucleus, and m_e is the electron mass. We use the known difference in mean-square charge radii between the different Pb isotopes [15] to separate our

measured values for the electronic shift into field and mass shift contributions. We find $V^B - V^X = 1.0(7) \times 10^{-5}$ fm^{-2}, and $\Delta^B - \Delta^X = 8.5(3.1) \times 10^{-6}$. The normal part of the mass shift (due to the change in the electron reduced mass) is negligibly small; hence the observed shift is a specific mass shift, due to electron correlations. This shift is unusually large, although similar shifts are known to occur in complex atoms [14].

In summary, we have measured some detailed spectroscopic parameters of the $X(0)(v=0)\rightarrow B(1)(v=5)$ transition of PbO. The measured value of the $B(1)$ state hfs provides an important data point for checking calculations of the effective electric field acting on an electron EDM in excited states of PbO.

[1] M. G. Kozlov and D. DeMille, Phys. Rev. Lett. **89**, 133001 (2002).

[2] T. A. Isaev, A. N. Petrov, N. S. Mosyagin, A. V. Titov, E. Eliav, and U. Kaldor, Phys. Rev. A **69**, 030501(R) (2004); A. N. Petrov, A. V. Titov, T. A. Isaev, N. S. Mosyagin, and D. DeMille, *ibid.* **72**, 022505 (2005).

[3] B. C. Regan, E. D. Commins, C. J. Schmidt, and D. DeMille, Phys. Rev. Lett. **88**, 071805 (2002).

[4] D. DeMille, F. Bay, S. Bickman, D. Kawall, D. Krause, Jr., S. E. Maxwell, and L. R. Hunter, Phys. Rev. A **61**, 052507 (2000); D. Kawall, F. Bay, S. Bickman, Y. Jiang, and D. DeMille, Phys. Rev. Lett. **92**, 133007 (2004).

[5] L. R. Hunter, S. E. Maxwell, K. A. Ulmer, N. D. Charney, S. K. Peck, D. Krause, Jr., S. Ter-Avetisyan, and D. DeMille, Phys. Rev. A **65**, 030501(R) (2002).

[6] D. Egorov, J. D. Weinstein, D. Patterson, B. Friedrich, and J.

M. Doyle, Phys. Rev. A **63**, 030501(R) (2001).

[7] A. S. Arnold, J. S. Wilson, and M. G. Boshier, Rev. Sci. Instrum. **69**, 1236 (1998); C. J. Hawthorn, K. P. Weber, and R. E. Scholtena, *ibid.* **72**, 4477 (2001).

[8] T. Watanabe and Y. Amako, J. Chem. Phys. **106**, 3891 (1997).

[9] F. Martin, R. Bacis, J. Vergès, J. Bachar, and S. Rosenwaks, Spectrochim. Acta **44A**, 889 (1988).

[10] H. G. Howell, Proc. R. Soc. London, Ser. A **153**, 683 (1936); E. A. Dorko *et al.*, Chem. Phys. **102**, 349 (1986).

[11] J. K. G. Watson, J. Mol. Spectrosc. **80**, 411 (1980).

[12] J. Schlembach and E. Tiemann, Chem. Phys. **68**, 21 (1982).

[13] H. Knöckel, U. Lindner, and E. Tiemann, Mol. Phys. **61**, 351 (1987).

[14] W. H. King, *Isotope Shifts in Atomic Spectra* (Plenum Press, New York, 1984).

[15] R. C. Thompson *et al.*, J. Phys. G **9**, 443 (1983).